Proc. Natl. Acad. Sci. USA
Vol. 82, pp. 3227–3231, May 1985
Biophysics

A neutron diffraction study on the location of the polyene chain of retinal in bacteriorhodopsin

(purple membrane/*Halobacterium halobium*/proton pump)

F. SEIFF, I. WALLAT, P. ERMANN*, AND M. P. HEYN

Biophysics Group, Department of Physics, Freie Universität Berlin, Arnimallee 14, D-1000 Berlin 33, Federal Republic of Germany

Communicated by M. A. El-Sayed, January 17, 1985

ABSTRACT **We report on the location of the chain part of the retinylidene chromophore in the projected density of bacteriorhodopsin as determined by neutron diffraction from the two-dimensional purple membrane lattice. For this purpose, partially deuterated retinal was synthesized containing 10 deuterons at positions C-8, C-10, C-12, C-14, C-19(3), and C-20(3) of the polyene chain. Two sets of dark-adapted samples were prepared in entirely different ways: (*i*) Deuterated retinal was incorporated biosynthetically during growth of the bacteria by using the mutant JW5, which is deficient in the synthesis of retinal. (*ii*) The chromophore was converted to retinal oxime, the resulting colorless apomembrane was regenerated with deuterated retinal, and the residual retinal oxime was removed by washing with bovine serum albumin. Characterization of these samples by x-ray diffraction, absorption, and flash spectroscopy showed that they were identical to native purple membrane samples as judged by these criteria. Fourier difference maps were calculated from the differences in in-plane diffraction from the deuterated membranes and from protonated samples that were prepared in exactly the same way. At 8.7 Å resolution, both maps show a single major peak at the same position with the center of mass of the labeled part of the chain (C-11) between helices 6 and 3 but closer to helix 6. It appears likely that the COOH-terminal helix G, to which retinal is attached at lysine-216, is either helix 2 or 6.**

The primary event in the function of the light-driven proton pump bacteriorhodopsin is the absorption of light by the retinylidene chromophore. The Schiff base linkage of the chromophore to lysine-216 of bacteriorhodopsin is also most likely involved in the subsequent events of proton transfer (1). Knowledge of the location of the chromophore is thus a prerequisite for any detailed model on the mechanism of bacteriorhodopsin. Since bacteriorhodopsin forms a two-dimensional hexagonal lattice in the plane of the purple membrane, a wealth of information has been obtained by using structural methods, in particular electron diffraction (2, 3). Thus far, the position of retinal could not yet be resolved by the latter method. In a pioneering study, King *et al.* (4) determined this location, projected onto the plane of the membrane, by means of neutron diffraction with perdeuterated retinal containing 28 deuterons. Three main peaks were observed in the Fourier difference map and an unambiguous assignment was difficult. Fluorescence energy transfer has also been used in an attempt to determine the in-plane position and orientation of the chromophore (5, 6). Recently, the work of King was repeated with a different sample preparation and significant improvements in the diffraction data (7). All four studies concluded that the chromophore is located in the interior of bacteriorhodopsin. A clear discrepancy exists between the results of King *et al.* (4) and Jubb *et al.* (7) concerning the location of the β-ionone ring. There is also considerable uncertainty about the positions of the chain and the Schiff base. Whereas in ref. 4 the Schiff base position was assigned to one of several peaks, in ref. 8 two distinct density regions were identified corresponding to the hydrocarbon chain. In contrast to the previous neutron diffraction work, which used perdeuterated retinal with 15 of 28 deuterons concentrated in the β-ionone ring and the remaining 13 stretched out along the long polyene side chain, we have used partially deuterated retinal with only 10 deuterons, which were concentrated in the middle of the polyene chain (see Fig. 1). Since the retinal molecule is ≈15 Å long in the all-*trans* form and makes an angle of ≈20° with the plane of the membrane (9), we labeled a site in the projected density of the membrane, which differs from that in the previous work. This site is, moreover, closer to the Schiff base linkage to lysine-216 of helix G, thus facilitating the assignment of helix G to one of the seven helices of the structure. Samples were prepared in two different ways. In the first procedure, the method of King was used (4) with one important modification: unlabeled retinal oxime was completely removed by washing with bovine serum albumin. In the second method, the partially deuterated retinal was added to the growth medium of the *Halobacterium halobium* mutant JW5, which is deficient in the synthesis of retinal. In this way, the labeled retinal was incorporated biosynthetically without the necessity of any of the possibly deleterious steps involved in the first procedure. With both methods, only a single major peak was observed in the density and the same position was found for the center of the polyene chain—close to helix 6 in the interior of bacteriorhodopsin. The problem of assigning the seven helical stretches in the sequence (A–G) to the seven helices observed in the structure (1–7; see Fig. 4) is still unsolved (10–13). At first sight, it appears that because of the lengths of the projected retinal chain and the lysine side chain to which it is attached, a unique assignment of helix G cannot be made. If we combine our result with that of previous diffraction work (7), however, the number of possibilities is reduced to two. It appears likely that G is either 2 or 6.

MATERIALS AND METHODS

Materials. All-*trans*-retinal (Fluka), hydroxylamine hydrochloride (Merck) and bovine serum albumin (fraction V, fatty acid-free; Serva, Heidelberg) were used without further purification.

Preparation of [$^2H_{10}$]Retinal. [8,10,12,14,19,19,19,20,20,20-$^2H_{10}$]Retinal (Fig. 1) was synthesized as described in detail (14). The 13-*cis*, 9-*cis*, and all-*trans* isomers of [$^2H_{10}$]retinal were separated by HPLC and characterized by mass spectroscopy, ^1H NMR, and UV spectroscopy. The mass spectrum showed one major peak (79%) at 294, and minor peaks at 293 (14%) and 295 (5%). The average number of deuterons

The publication costs of this article were defrayed in part by page charge payment. This article must therefore be hereby marked "*advertisement*" in accordance with 18 U.S.C. §1734 solely to indicate this fact.

*Present address: vcn Heyden GmbH, D-8400 Regensburg, Federal Republic of Germany.

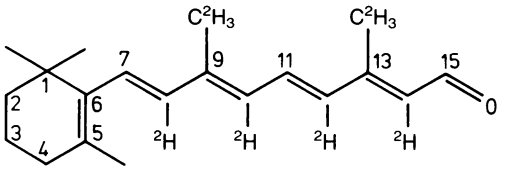

FIG. 1. Structure of the synthetic [$^2H_{10}$]retinal.

incorporated was 9.94. The ^1H NMR spectrum of [$^2H_{10}$]-retinal showed three peaks for protons in the polyene chain that were assigned to the three protons at C-15, C-11, and C-7 and that occurred at the same chemical shift values as for fully protonated retinal. The UV spectrum in ethanol had its maximum at 380 nm and was identical to the spectrum for protonated retinal.

Regeneration of Apomembrane (S9 Sample). Purple membranes from strain S9 were converted into colorless apomembranes containing retinal oxime by irradiation with light (>520 nm) in the presence of hydroxylamine (15). The absorption spectrum of the apomembrane suspension had no residual absorbance at 570 nm, showing that the reaction had gone to completion. The apomembranes were regenerated with either all-*trans*-[$^2H_{10}$]retinal or with protonated all-*trans*-retinal in ethanol. Apomembrane suspensions were titrated spectroscopically until the excess retinal became observable at 380 nm. The final amount of ethanol never exceeded 1% (vol/vol). Retinal oxime and excess retinal were removed by washing seven times with bovine serum albumin (16). Residual albumin was removed by washing twice with distilled water. The absorption spectrum of the final product shows no absorbance at 380 nm due to retinal oxime or excess retinal (Fig. 2*a*). The percentage regeneration calculated from the absorbance at 570 nm was 95%. The ratio of absorbance at 280 and 570 nm (1.8) was the normal

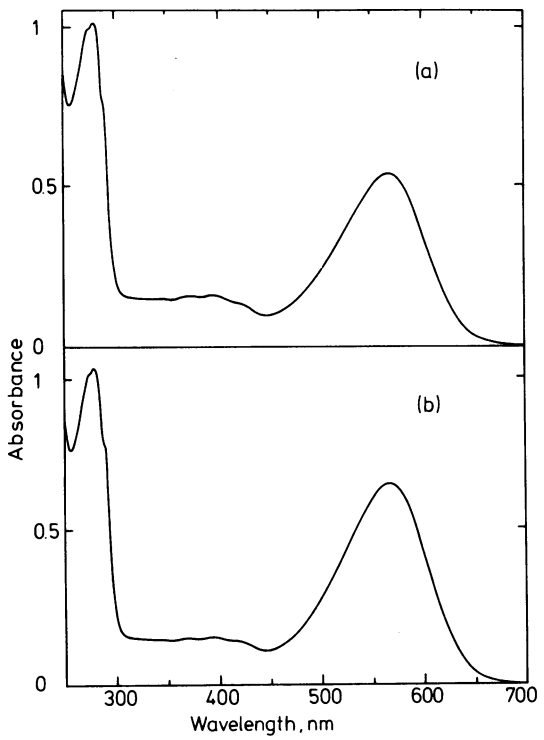

FIG. 2. Absorption spectra of suspensions of light-adapted purple membranes reconstituted with [$^2H_{10}$]retinal. Spectra were taken with a Shimadzu 240-UV spectrophotometer with integrating sphere. (*a*) Strain S9 after removal of retinal oxime by washing with bovine serum albumin. (*b*) The retinal$^-$ mutant JW5 after regeneration with retinal during growth of bacteria.

range for purple membranes and indicated that no residual albumin remained adsorbed to the membranes. The x-ray diffraction pattern of these regenerated membranes was, except for somewhat broader reflections, identical to that of native purple membranes.

Regeneration of Retinal$^-$ Mutants (JW5 Sample). The mutant strain JW5, which is deficient in the synthesis of retinal, was grown under standard conditions. On days 4, 5, and 6 of growth, all-*trans*-[$^2H_{10}$]retinal or fully protonated retinal was added to the growth medium (17). The absorption spectrum of the resulting purple membranes (Fig. 2*b*) has the same ratio of absorbance at 280 and 570 nm (1.6) as native purple membrane and shows no sign of additional absorbance at ≈420 nm from a cytochrome *b*-type protein. To test whether all the available sites in the lattice were occupied by retinal, additional retinal was added to the isolated membrane patches. No further increase in absorbance at 570 nm was observed. Of the retinal added to the growth medium, 25% was incorporated in purple membranes. The mean patch diameter, as determined from the flash-induced transient dichroism, was ≈1 μm. The x-ray diffraction pattern of these samples was, accordingly, sharper and better resolved than for wild-type purple membranes.

Neutron Diffraction Experiments. Oriented purple membrane samples were prepared for neutron diffraction by applying a concentrated suspension on a thin quartz slide (0.3 mm) and by allowing it to dry slowly (24 hr) at 50% relative humidity. The resulting films covered an area of 8 × 20 mm and contained 9 mg of bacteriorhodopsin. Each slide was coated with purple membrane in this way on both sides. Ten slides formed a stack of total thickness 6 mm, containing 180 mg of bacteriorhodopsin. This stack was mounted in an aluminum sample holder. The neutron diffraction data were collected on the D16 diffractometer of the High Flux Reactor (Institut Laue-Langevin, Grenoble). A detailed description of this instrument has recently appeared (18). Briefly, a neutron beam of wavelength 4.52 Å is selected by a graphite monochromator. The sample stack is mounted on the θ-axis of the diffractometer with the normal to the quartz planes initially (θ = 0) parallel to the incident beam. Data were collected in a (θ, 2θ) scan in which the detector was moved in small angular steps synchronously with the sample, in such a way that the angular position of the detector (2θ) is always twice that of the sample (θ). The angular resolution of the detector was 0.145°. Since the purple membranes are stacked parallel to the quartz slides but are randomly oriented around the axis perpendicular to the slide, the (θ, 2θ) scan provides a powder pattern of the in-plane diffraction from the two-dimensional bacteriorhodopsin lattice. The diffracted intensities were detected by a two-dimensional position-sensitive detector (7). The quality of the parallel orientation of purple membranes on the slides was determined by measuring the mosaic spread of the first-order lamellar diffraction. For the two JW5 samples, a full width at half height of 12° was obtained, indicating excellent orientation. For the S9 samples, the mosaic spread was 16°. Data collection times were 29 hr for each of the S9 samples and 66 hr for each of the JW5 samples. The data were collected at room temperature and 50% relative humidity in the dark-adapted state of bacteriorhodopsin.

RESULTS

Fig. 3 shows the raw intensity data from the position-sensitive detector for the JW5 sample (*a*, deuterated; *b*, protonated). Similar data were obtained for the S9 sample. The observed intensities could be indexed on a hexagonal lattice and the corresponding (*h*, *k*) reflection indices are indicated. The (7,1) peak is the highest reflection observed. The (3,3), (4,4), and (6,0) reflections are missing. Since only 10 protons

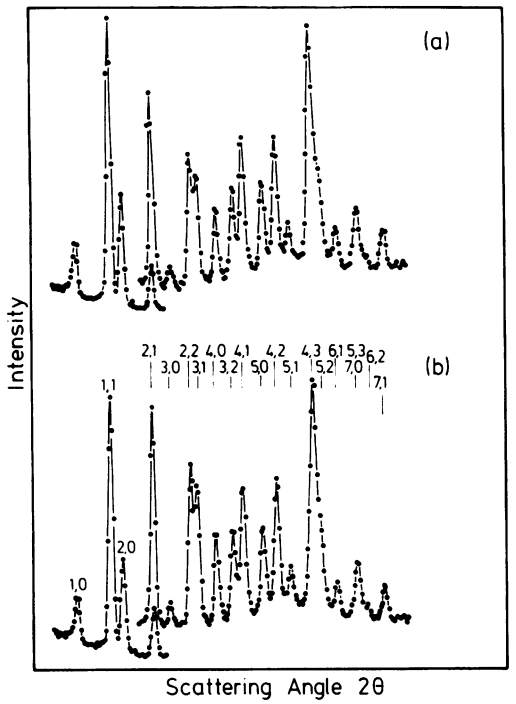

FIG. 3. Neutron diffraction intensities of oriented purple membranes from regenerated JW5 mutants as a function of the detector angle 2θ. Starting with the (2,1) reflection, the vertical scale has been expanded by a factor of 4.5. (*a*) Reconstituted with [$^2H_{10}$]retinal. (*b*) Reconstituted with protonated retinal. Shown are the outputs of the position-sensitive detector. No scaling or background subtraction has been applied. Both samples were in the beam for the same number of monitor counts. The reflections are indexed on the basis of a hexagonal lattice. From left to right, 2θ ranges from 0° to 50°.

are replaced by deuterons, small intensity differences are expected. By comparing Fig. 3 *a* and *b*, clear changes can nevertheless be observed in the (1,1), (2,0), (2,2), (3,1), and (4,0) reflections. The background due to an identical stack of 10 quartz slides was measured but shown to be negligible. The background due to the incoherent scattering of the sample was subtracted and the integrated intensities were corrected by a Lorentz factor of $(h^2 + hk + k^2)^{1/2}$, which is appropriate for a well oriented sample with a mosaic spread of 12° (10). It is important to note that the mosaic spread was identical in the protonated and deuterated samples, so that both data sets were corrected by the same Lorentz factor. The absorption and projection corrections were shown to be negligible (7). The intensity $I(r)$ was split into the two squared structure factors $F^2(h, k)$ with $h^2 + hk + k^2 = r$ according to their ratios in the electron diffraction data (2). This approximation and the use of phase information from electron microscopy have been discussed in detail elsewhere (4, 7, 11). Model calculations show that the conditions under which these approximations are valid are satisfied in the present case (G. Büldt and H.-J. Plöhn, personal communication). Since the change in total scattering power of the unit cell due to the replacement of 10 protons by 10 deuterons is very small, the structure factors were scaled in such a way that the sum of the intensities of the protonated and deuterated samples became equal (19). For the JW5 samples, the two sums differed only by 1.6%; for the S9 samples, they differed by 6%. Since protonated and deuterated samples were in the beam for the same number of monitor counts and care was taken to prepare the two samples in exactly the same way, scaling factors close to 1 were expected. The main source of these differences resides in the difficulty of applying the same amount of material to the same area on the quartz slides. The final structure factor moduli for the protonated (F_P) and deuterated (F_D) samples used in the Fourier synthesis are collected in Table 1 together with the phases from the electron microscopy data (2). The native projected structure based on all the reflections up to and including (5,2) is shown in Fig. 4. Superimposed on the native structure are shown the

Table 1. Structure factors and phases for protonated (P) and deuterated (D) samples from JW5 and S9 preparations

		JW5		S9		Phase,
h	*k*	F_P	F_D	F_P	F_D	radians
1	0	62.5	69.6	92.0	105.4	5.97
1	1	194.2	208.9	255.6	272.5	2.83
2	0	128.1	142.5	161.6	182.5	3.32
2	1	46.4	42.8	56.4	49.0	3.67
1	2	96.2	88.8	116.9	101.7	5.45
3	0	42.4	42.4	39.0	39.0	1.68
2	2	106.9	93.0	129.8	116.2	2.06
3	1	97.3	83.9	125.8	108.8	3.28
1	3	25.2	21.7	32.6	28.2	2.09
4	0	87.2	75.2	97.7	84.9	4.92
3	2	74.1	74.1	88.6	90.8	0.09
2	3	48.6	48.6	58.1	59.5	5.97
4	1	88.5	88.5	99.8	97.8	5.55
1	4	67.4	67.4	75.9	74.5	5.38
5	0	94.9	94.9	109.2	120.5	6.02
4	2	36.8	36.8	41.3	37.6	1.80
2	4	108.9	108.9	122.3	111.1	4.19
5	1	19.2	19.2	15.0	15.0	0.49
1	5	72.1	72.1	51.0	51.0	4.68
4	3	139.1	141.6	155.9	149.7	2.18
3	4	86.2	87.8	96.6	92.7	2.83
5	2	89.7	89.7	113.1	98.2	2.27
2	5	36.3	36.3	45.8	39.8	4.75

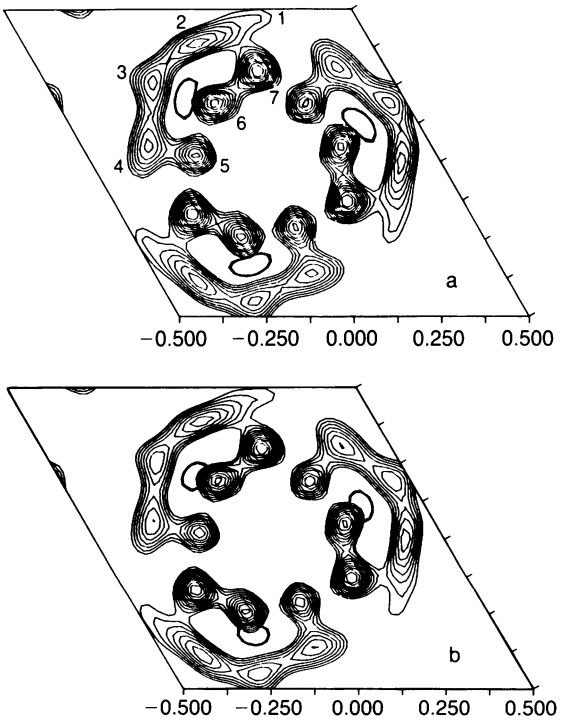

FIG. 4. Projected density of the purple membrane as determined from the neutron diffraction intensities and electron microscopy phases at 8.7 Å resolution. Negative contours have been omitted. The side of the hexagonal unit cell corresponds to 63 Å. Superimposed on the structures are the 83% contour lines from the Fourier difference maps for the retinal chain position (see Fig. 5). (*a*) S9 sample. (*b*) JW5 sample.

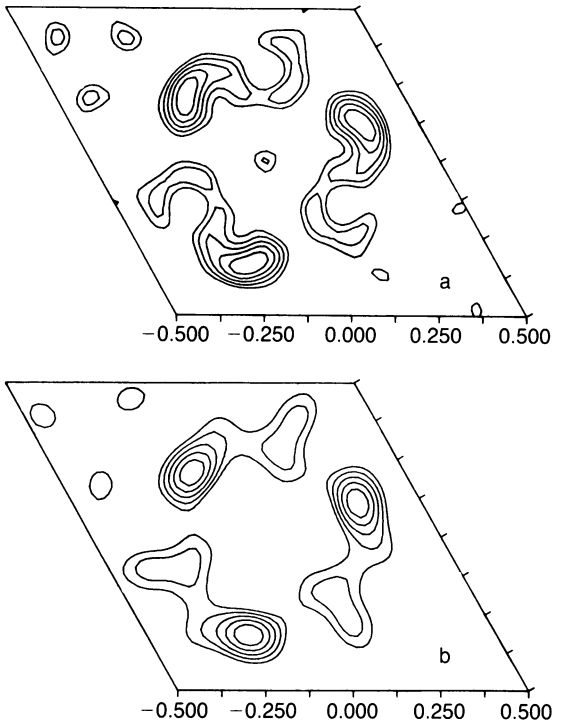

FIG. 5. Fourier difference maps for the location of the retinal polyene chain. (*a*) S9 sample. (*b*) JW5 sample. Only positive contours are shown. The same phases were used as in Fig. 4 for the native structure.

83% contour lines from the Fourier difference maps for the retinal position of Fig. 5 (*a*, S9 sample; *b*, JW5 sample). Since no intensity changes were observed in the reflections beyond (5,2), both the native and the Fourier difference maps were calculated at this resolution of 8.7 Å. Use of a slightly different set of phases and structure factor ratios (3) makes no significant difference in the structure at this resolution. It is clear from Fig. 4 that the projected structure determined from the neutron diffraction data is the same in all its main features as the well known structure from electron diffraction (2,3). For clarity, only the 11 positive contour lines are shown ranging in steps of 5% from 45% to 95% of the density. By using the differences in structure factors between deuterated and protonated samples and the same phases and ratios for superimposed reflections as were used before in the calculation of the native structure (2), Fourier difference plots were calculated. All the reflections listed in Table 1 were included in the calculation. The results are shown in Fig. 5 *a* (S9 sample) and *b* (JW5 sample). Again, only the 5 positive contour lines are shown, ranging in steps of 16.7% from 0% (not shown) to 100% (not shown) of the difference density. The plots show one strong maximum per molecule for both samples at very nearly the same position, which is more than twice as high as the next maximum. Thus, two entirely different preparation methods lead to the same location for the polyene chain. The 83% contour lines from Fig. 5 are redrawn in Fig. 4 superimposed on the native structure. It is clear that the center of mass of the chain deuteration (C-11) is located between helices 3 and 6 and adjacent to helix 6.

DISCUSSION

The change in scattering power when only 10 protons are replaced by 10 deuterons in a structure of molecular weight 26,800 is unusually small. For this reason, and to correct for the possibility that the preparation procedures could have affected the structure of bacteriorhodopsin and the quality of the lattice in some minor way, we attempted to prepare the protonated and deuterated samples in exactly the same way. Rather than use native purple membranes for the protonated samples, we prepared 180 mg of both the S9 and JW5 samples in the same laborious way as for the deuterated samples. We measured the diffraction patterns for deuterated and protonated samples during the same machine run, in the same beam geometry, and with equal counting statistics. Sample quality was judged by absorption spectroscopy (Fig. 2), flash photolysis, and x-ray diffraction (data not shown). On the basis of these criteria, the deuterated and protonated samples were judged to be equal and to be indistinguishable from native purple membranes.

Our preparation methods represent significant improvements over previous work. We showed that King's bleaching method gives good results, provided that retinal oxime is removed immediately after regeneration. It seemed worthwhile, however, to try to prepare samples that were not exposed to many hours of irradiation in the presence of 1.4 M hydroxylamine and that were not handled by exhaustive washing with bovine serum albumin. The recent method of Jubb *et al.* (7), in which retinal synthesis is suppressed by the addition of nicotine and in which a cocktail of oxidation products of β-carotene is added during bacterial growth, is a significant step forward in this direction. Unfortunately, this mixture contained many retinal analogs of longer and shorter chain lengths in addition to the deuterated retinal. The absorption spectrum (see ref. 7) showed unusually high absorbance between 300 and 450 nm, in the correct range for free retinal analogs, indicating that a considerable amount of these analogs had been incorporated in the membranes. Whether they contribute to the observed neutron diffraction is uncertain. It is well-known, however, that analogs of slightly longer or shorter chain lengths bind to the retinal binding site (20, 21). Indirect evidence for competition for the binding site by these analogs is provided by the very low percentage of incorporation of deuterated retinal (5%). To overcome these problems, we used a retinal$^-$ mutant and regenerated with protonated or [$^2H_{10}$]retinal only. Fig. 2 shows that no additional absorbance occurs between 300 and 450 nm. The ratio of absorbance at 280 and 570 nm indicates that the normal amount of retinal was incorporated. Addition of external retinal to these membranes did not lead to an increase in absorbance at 570 nm. It is reassuring to see (Figs. 4 and 5) that these two widely differing preparation methods lead, within experimental error, to the same location for the center of mass of the polyene chain.

Our data are compatible with those of Jubb *et al.* (7) in the sense that neither of us observed the (3,3) and (6,0) reflections that were observed by King *et al.* (4). We note that the (3,3) and (6,0) reflections are also absent in the x-ray diffraction pattern (22) and that the intensity ratios in the x-ray and neutron diffraction patterns are remarkably similar. In the electron diffraction data, these reflections are very weak. King *et al.* observed the largest change in intensity in the (3,3) reflection (G. I. King, personal communication) and very large changes in the (4,3) and (5,2) reflections which were not observed in this magnitude by Jubb *et al.* and by us. In all three studies, large changes were observed in the (4,0) reflection. In our work, the sign of this change is the same as observed by Jubb *et al.* and opposite that observed by King *et al.* Although our data are clearly in better agreement with those of Jubb *et al.*, they are not the same, which is to be expected because we labeled only the retinal chain. From linear dichroism measurements, it is known that the orientation of the retinal chain in the all-*trans* form makes an angle of ≈20° with the plane of the membrane (9). The projection of the chain onto the membrane thus has a length of ≈14 Å. Comparison of the Fourier difference maps shows (Fig. 6) that our position for the center of deuteration of the polyene chain (C-11) is ≈4 Å away from Jubb's position for the center

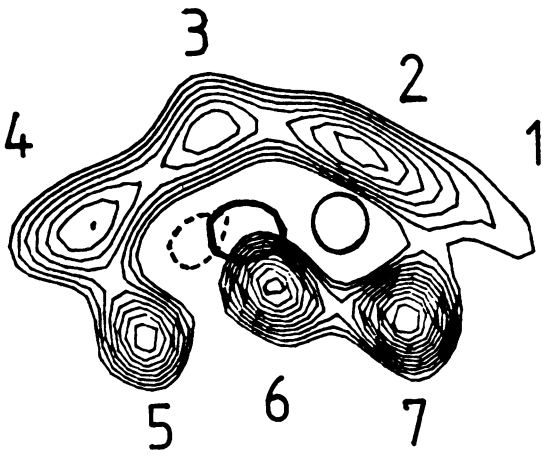

FIG. 6. Comparison of the neutron diffraction results on the location of the retinal. In the interior of bacteriorhodopsin, three closed contours are shown in heavy lining. Contour at right, main peak of King *et al.* (4), assigned to the β-ionone ring; middle contour, result of this study for the center of deuteration of the chain (C-11, JW5 sample); contour at left (---), result from Jubb *et al.* (7) corresponding to the center of deuteration of retinal (C-7, C-8).

of deuteration of the entire retinal (between C-7 and C-8 of the chain). This is close to the expected projected distance between these two points if the polyene chain is inclined by 20° to the plane of the membrane. The results of these two studies thus fit together well. The position of the Schiff's base nitrogen may now be estimated by continuing for the appropriate distance along the line through Jubb's maximum and ours. On the basis of this analysis, the Schiff's base nitrogen is located roughly halfway between helices 2 and 6.

Taking into account the possibility that the lysine sidechain may be fully extended in the plane of the membrane, one concludes that lysine-216 and helix G can only be assigned to helix 2 or 6 of the structure. This assignment is consistent with diffraction results (10), but it does not fit with recent model calculations that assign G to helix 4 (11). As discussed above, our diffraction data are not compatible with those of King *et al.*, who found three maxima and assigned the largest near helix 2 to the β-ionone ring (Fig. 6). The distance between our position for the middle of the chain and theirs for the ring is, however, also consistent with expectations for a projected retinal making an angle of 20° with the membrane. Since they observed positive density in the area of our maximum that was associated with the chain (8), we cannot exclude the possibility that the retinal extends from the Fourier difference peak at the right (ring) in the direction of helices 4 and 5. In view of the close similarity of our intensity data with those of Jubb *et al.*, we feel, however, that the first assignment is most likely to be correct, implying that the COOH-terminal helix is either helix 2 or 6. Experiments with a deuterated β-ionone ring will lead to a conclusive assignment.

We thank R. Henderson and R. Stroud for providing us with the phases and structure factor ratios from their electron diffraction work. We are grateful to G. Büldt, W. Sperling, and G. Zaccai for helpful discussions and advice; to H. Otto and S. Grzesiek for assistance with computing and plotting programs; to J. Weber and D. Oesterhelt for providing us with strain JW5; and to the staff of the D16 diffractometer of the Institut Laue-Langevin, Grenoble, for excellent technical support. This work was generously supported by Grant 03 B72C01 9 of the Bundesministerium für Forschung und Technologie.

1. Stoeckenius, W. & Bogomolni, R. A. (1982) *Annu. Rev. Biochem.* **52,** 587–616.
2. Unwin, P. N. T. & Henderson, R. (1975) *J. Mol. Biol.* **94,** 425–440.
3. Hayward, S. B. & Stroud, R. M. (1981) *J. Mol. Biol.* **151,** 491–517.
4. King, G. I., Mowery, P. C., Stoeckenius, W., Crespi, H. L. & Schoenborn, B. P. (1980) *Proc. Natl. Acad. Sci. USA* **77,** 4726–4730.
5. Kouyama, T., Kimura, Y., Kinosita, K. & Ikegami, A. (1982) *J. Mol. Biol.* **153,** 337–359.
6. Rehorek, M., Dencher, N. A. & Heyn, M. P. (1983) *Biophys. J.* **43,** 39–45.
7. Jubb, J. S., Worcester, D. L., Crespi, H. L. & Zaccai, G. (1984) *EMBO J.* **3,** 1455–1461.
8. King, G. (1984) *Biophys. J.* **45,** 210a (abstr.).
9. Heyn, M. P., Cherry, R. J. & Mueller, U. (1977) *J. Mol. Biol.* **117,** 607–620.
10. Wallace, B. A. & Henderson, R. (1982) *Biophys. J.* **39,** 233–239.
11. Trewhella, J., Anderson, S., Fox, R., Gogol, E., Khan, S., Zaccai, G. & Engelman, D. M. (1983) *Biophys. J.* **42,** 233–241.
12. Engelman, D. M., Henderson, R., McLachlan, A. D. & Wallace, B. A. (1980) *Proc. Natl. Acad. Sci. USA* **77,** 2023–2027.
13. Agard, D. A. & Stroud, R. M. (1982) *Biophys. J.* **37,** 589–602.
14. Ermann, P. (1982) Dissertation (Universitaet Erlangen-Nuernberg, F.R.G.).
15. Rehorek, M. & Heyn, M. P. (1979) *Biochemistry* **18,** 4977–4983.
16. Katre, N. V., Wolber, P. K., Stoeckenius, W. & Stroud, R. M. (1981) *Proc. Natl. Acad. Sci. USA* **78,** 4068–4072.
17. Oesterhelt, D. (1982) *Methods Enzymol.* **88,** 10–17.
18. Institut Laue-Langevin (1983) *Neutron Beam Facilities at the HFR*, available from the Scientific Secretary, Institut Laue-Langevin, 156X, 38042 Grenoble Cedex, France.
19. Blundell, T. L. & Johnson, L. N. (1976) *Protein Crystallography* (Academic, New York).
20. Tokunaga, F., Govindjee, R., Ebrey, T. G. & Crouch, R. (1977) *Biophys. J.* **19,** 191–198.
21. Ovchinnikov, Yu. A., Shkrob, A. M., Rodionov, A. V. & Mitzner, B. I. (1979) *FEBS Lett.* **97,** 15–19.
22. Henderson, R. (1975) *J. Mol. Biol.* **93,** 123–138.